Helical Structures

DOI: 10.1002/anie.200904614

Intermetallic Interactions Within Solvated Polynuclear Complexes: A Misunderstood Concept**

Natalia Dalla Favera, Ulf Kiehne, Jens Bunzen, Sophie Hytteballe, Arne Lützen, and Claude Piguet**

For polynuclear gas-phase $[M_mL_n]^{z+}$ complexes comprising cationic metals and neutral ligands, the simple use of the Coulomb equation [Eq. (1)] usually gives a preliminary but

$$\Delta E_{gas}^{M,M} = \frac{z_1 z_2 e^2 N_{Av}}{4\pi\varepsilon_0\varepsilon_r d} \quad (1)$$

satisfying estimation of the pair intramolecular intermetallic repulsions $\Delta E_{gas}^{M,M}$, which limit the stability of the final (supra)molecular architectures (z_1 and z_2 are the effective charges in electrostatic units borne by the two metals considered as point charges, $e = 1.602\times10^{-19}$ C is the elemental electric charge, $N_{Av} = 6.023\times10^{-23}$ mol^{-1} is Avogadro's number, $\varepsilon_0 = 8.859\times10^{-19}$ C V^{-1} m^{-1} is the permittivity of vacuum, $\varepsilon_r = 1$ is the relative permittivity in the gas phase and in the molecule,[1] and d is the separation between the interacting metals). A more refined energetic balance includes polarization and covalent effects, which eventually rationalizes the stability of charged complexes detected by electrospray mass spectrometry in the gas phase (ESI-MS).[2]

The same argument is frequently invoked to address the stability of these supramolecular complexes in solution, which is where the majority of self-assembly processes occur.[3] However, this approach neglects the changes in solvation energies $\Delta_{solv}G_x^0$ that result from the complexation of additional components in the final complexes x.[4] For the pair of cationic metals considered in Equation (1), the global solvation energy of the final complex can be roughly approximated by using the Born Equation [Eq. (2)], in which R_x is the

$$\Delta_{solv}G_x^0 = -\frac{(z_1+z_2)^2 e^2 N_{Av}}{8\pi\varepsilon_0 R_x}\left(1-\frac{1}{\varepsilon_r^{solv}}\right) \quad (2)$$

pseudo-spherical Born radius deduced from the van der Waals[5] or from the Connolly volumes[6] of the final complex, and ε_r^{solv} is the relative permittivity of the solvent.

The recent application of the site-binding model [Eq. (3)][7] for modeling the two-component self-assembly

$$\beta_{m,n}^{M,L} = \omega_{chir}^{M,L}\omega_{m,n}^{M,L}\prod_{i=1}^{mn}(f_i^{M,L})\prod_{i=1}^{mn-m-n+1}(c_i^{eff})\prod_k''(u_k^{M,M})\prod_l'''(u_l^{L,L}) \quad (3)$$

processes that lead to polynuclear lanthanide helicates [Eq. (4)] gave estimations for the three different intermetallic

$$m\,M^{z+} + n\,L \rightleftharpoons [M_mL_n]^{m\,z+} \quad \beta_{m,n}^{M,L} \quad (4)$$

interactions $\Delta E_{sol}^{M,M}$ (Figure 1), which cannot be explained by the sole use of Coulomb interactions ($\omega_{chir}^{M,L}\omega_{m,n}^{M,L}$ is the statistical factor of the assembly,[8] $f_i^{M,L}$ is the intermolecular

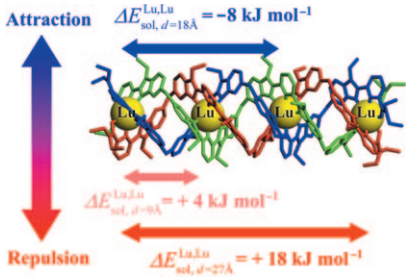

Figure 1. Experimental intramolecular intermetallic interactions $\Delta E_{sol,d}^{M,M}$ that operate between pairs of trivalent lanthanides within the triple-stranded helicate $[Lu_4(L)_3]^{12+}$ in acetonitrile (deduced with [Eq. (3)]).[9]

microscopic affinity that characterizes the connection of a metal M to the binding site i of a ligand L (including desolvation), c^{eff} is the effective concentration that corrects $f_i^{M,L}$ for intramolecular macrocyclization complexation processes, and $u_k^{M,M} = \exp(-\Delta E_k^{M,M}/RT)$ and $u_l^{L,L} = \exp(-\Delta E_l^{L,L}/RT)$ are the Boltzmann factors that account for the intermetallic $\Delta E_k^{M,M}$ and interligand $\Delta E_l^{L,L}$ interactions).[9]

Moreover, the thermodynamic interpretation of intramolecular intermetallic interactions in these tetranuclear lanthanide helicates is partially obscured by the screening effects produced by the four aligned triply charged cations. A more convincing and unambiguous proof for a chemically sensitive interpretation of the apparent intermetallic interactions that operates within complexes in solution requires a system in which $\Delta E_{sol}^{M,M}$ can be simply correlated with increasing intermetallic separation, and all other parameters

[*] Dr. U. Kiehne, J. Bunzen, S. Hytteballe, Prof. Dr. A. Lützen
Rheinische Friedrich-Wilhelms-Universität Bonn
Kekulé-Institut für Organische Chemie und Biochemie
Gerhard-Domagk-Strasse 1, 53121 Bonn (Germany)
E-mail: arne.luetzen@uni-bonn.de
N. Dalla Favera, Prof. Dr. C. Piguet
Department of Inorganic, Analytical and Applied Chemistry
University of Geneva
30 quai E. Ansermet, 1211 Geneva 4 (Switzerland)
E-mail: claude.piguet@unige.ch

[**] This work was supported through grants of the Swiss National Science Foundation and the Deutsche Forschungsgemeinschaft (SFB 624).

Supporting information for this article is available on the WWW under http://dx.doi.org/10.1002/anie.200904614.

are constants. This situation indeed occurs in the remarkable diastereoselective self-assembly of the D_2-symmetrical double-stranded helicates $[M_2(\mathbf{L}k)_2]^{2+}$ ($M = Cu^I$, Ag^I, $k = 1$–3, Figure 2), in which the C_2-symmetrical Tröger's base spacer of the ligand **L***k* can be extended in a stepwise fashion by successive introduction of additional rigid alkynyl groups so that the binding units and the symmetry of the molecular edifices are not modified.[10]

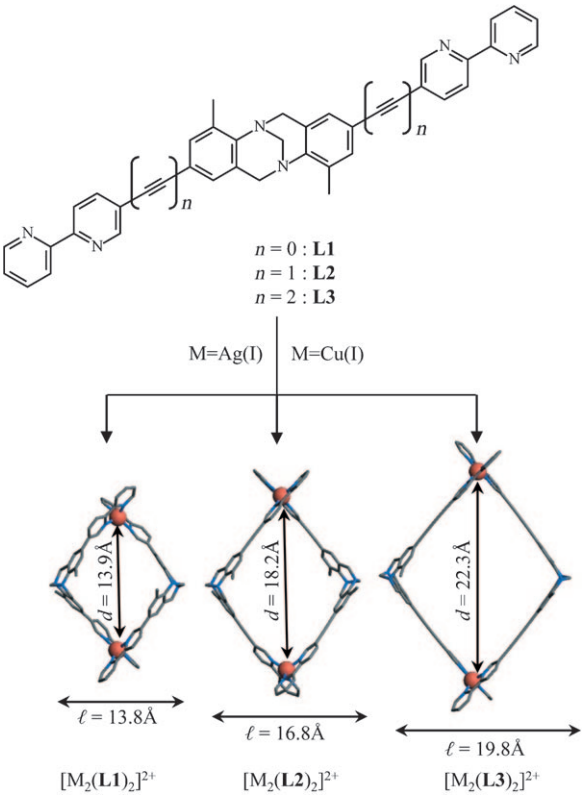

Figure 2. Diastereoselective formation of the double-stranded helicates $[M_2(\mathbf{L}k)_2]^{2+}$. The geometry of the complexes correspond to PM3-TM minimized structures for $M = Cu^I$.[10]

ESI-MS and ^{1}H NMR data recorded in dichloromethane/acetonitrile (5:1) confirm the formation of $[M_2(\mathbf{L}k)_2]^{2+}$ ($k =$ 1–3) as the major reaction products, together with some minor quantities of $[M_2(\mathbf{L}k)]^{2+}$ and $[M(\mathbf{L}k)_2]^{+}$ that are detected when the stoichiometric $|M_{tot}|/|\mathbf{L}k_{tot}|$ ratio is larger and smaller than 1.0, respectively.[10] The translational self-diffusion coefficients of $[M_2(\mathbf{L}k)_2]^{2+}$ obtained by diffusion-ordered spectroscopy (DOSY NMR in CD_2Cl_2/CD_3CN (5:1) at 293 K) translate into hydrodynamic volumes (V_H^x) that are comparable with the Connolly volumes (V_{Conn}^x) calculated from molecular modeling studies. This result implies that these complexes exist as discrete binuclear units in solution (Table S1 in the Supporting Information). Moreover, the discrepancies between V_H^x and V_{Conn}^x can be quantitatively assigned to the effective toroidal shape of the complexes, thus implying that the optimized gas-phase structures (Figure 2) are retained in solution (Figure S1 and Appendix 1 in the Supporting Information).[11]

Spectrophotometric titrations of **L***k* ($k = 1$–3) with $[Cu(CH_3CN)_4]PF_6$ or $AgClO_4$ in CH_2Cl_2/CH_3CN (5:1) show pronounced end points for $M:\mathbf{L}k = 1.0$, which correspond to the formation of $[M_2(\mathbf{L}k)_2]^{2+}$ as the major products. Specific variations of the molar extinction coefficients during the titrations prevent the observation of isosbestic points, which indicates the formation of small quantities of additional complexes with different stoichiometries (Figure S2–S4 in the Supporting Information). Factor analysis combined with non-linear least-squares techniques converge to the equilibria in Equations (5) and (6) for **L1** and **L2**, but to the equilibria in Equations (6) and (7) for **L3** (Table 1).

$$2\,[M(CH_3CN)_4]^+ + \mathbf{L}k \rightleftharpoons [M_2(\mathbf{L}k)(CH_3CN)_4]^{2+} + 4\,CH_3CN \quad \beta_{2,1}^{M,\mathbf{L}k} \tag{5}$$

$$2\,[M(CH_3CN)_4]^+ + 2\,\mathbf{L}k \rightleftharpoons [M_2(\mathbf{L}k)_2]^{2+} + 8\,CH_3CN \quad \beta_{2,2}^{M,\mathbf{L}k} \tag{6}$$

$$[M(CH_3CN)_4]^+ + 2\,\mathbf{L}k \rightleftharpoons [M(\mathbf{L}k)_2]^{+} + 4\,CH_3CN \quad \beta_{1,2}^{M,\mathbf{L}k} \tag{7}$$

Table 1: Experimental cumulative thermodynamic constants.[a]

Ligand	M	$\log(\beta_{2,1}^{M,\mathbf{L}k})$	$\log(\beta_{2,2}^{M,\mathbf{L}k})$	$\log(\beta_{1,2}^{M,\mathbf{L}k})$
L1	Cu^I	13.4(6)	19.5(6)	–
L2	Cu^I	11.9(4)	17.9(4)	–
L3	Cu^I	–	15.6(3)	10.8(3)
L1	Ag^I	13.2(4)	18.9(4)	–
L2	Ag^I	10.3(3)	15.6(4)	–
L3	Ag^I	–	12.0[b]	8.0[b]

[a] Obtained from the spectrophotometric titrations of **L***k* with $[M(CH_3CN)_4]^+$ in CH_2Cl_2/CH_3CN (5:1) at 293 K. [b] Estimated as their maximum values by simulation of the speciation using the HYSS program because of the weak spectrophotometric variations for the titration of **L3** with $[Ag(CH_3CN)_4]^+$ at 10^{-4} M.

Application of the site binding model [Eq. (3), see also Appendix 2 in the Supporting information] to the equilibria in Equations (5)–(7), gives Equations (8)–10, from which fits to the six experimental cumulative constants ($k = 1$–3) collected for each metal (Table 1 and Eqs S9–S14 and Appendix 2 in the Supporting Information), eventually provide two sets of six microscopic thermodynamic descriptors (Table 2).

$$\beta_{2,1}^{M,\mathbf{L}k} = 144\,(f_{N2}^{M})^2 u_{\mathbf{L}k}^{M,M} \tag{8}$$

$$\beta_{2,2}^{M,\mathbf{L}k} = 72\,(f_{N2}^{M})^4 u_{\mathbf{L}k}^{M,M} (u^{L,L})^2 c_{M,\mathbf{L}1}^{eff} (d_k/d_1)^{-3} \tag{9}$$

$$\beta_{1,2}^{M,\mathbf{L}k} = 12\,(f_{N2}^{M})^2 u^{L,L} \tag{10}$$

As expected, the microscopic affinity of the bipyridine binding units for Cu^I ($\Delta G_{N2}^{Cu} = -RT\ln(f_{N2}^{Cu}) = -38$ kJ mol^{-1}) is larger than that found for Ag^I cations ($\Delta G_{N2}^{Ag} = -25$ kJ mol^{-1}). The effective concentrations that measure the preorganization of the ligand strands for the intramolecular connection that produces the macrocyclic binuclear double-stranded complex $[M_2(\mathbf{L1})_2]^{2+}$ are the largest reported to date for helicates ($1.5 \le c_{M,L1}^{eff} \le 5$ M for M = Cu, Ag), the previous record being that of the tricopper double-stranded helicates ($c_{Cu}^{eff} = 1.3$ M) reported by Lehn and co-workers.[12b] This result

Table 2: Fitted microscopic thermodynamic parameters for the self-assembly of $[M_m(\mathbf{Lk})_n]^{m+}$ ($M = Cu^I$, Ag^I; $k = 1$–3).[a]

Parameter[b]	$M = Cu^I$	$M = Ag^I$
$\log(f_{N2}^{M})/\Delta G_{N2}^{M}$ [c]	6.6/−38	4.3/−25
$\log(c_{M,L1}^{eff})/\Delta G_{corr}^{M,L1}$ [d]	0.18/−1	0.7/−4
$\log(u^{L,L})/\Delta E^{L,L}$ [e]	−3.5/20	−1.6/9.4
$\log(u_{L1}^{M,M})/\Delta E_{L1}^{M,M}$ [f]	−2/11	2.5/−14
$\log(u_{L2}^{M,M})/\Delta E_{L2}^{M,M}$ [f]	−3.5/20	−0.4/2.4
$\log(u_{L3}^{M,M})/\Delta E_{L3}^{M,M}$ [f]	−5.7/33	−3.9/22

[a] Measured in CH_2Cl_2/CH_3CN (5:1) at 293 K. Since six parameters are fitted to Equations S9–S14 (Appendix 2 in the Supporting Information), there are no uncertainties. [b] ΔG and ΔE values given in [kJ mol^{-1}]. [c] $\Delta G_{N2}^{M} = -2.303RT\log(f_{N2}^{M})$. [d] $\Delta G_{corr}^{L,M1} = -2.303RT\log(c_{M,L1}^{eff})$. [e] $\Delta E^{L,L} = -2.303RT\log(u^{L,L})$. [f] $\Delta E_{Lk}^{M,M} = -2.303RT\log(u_{Lk}^{M,M})$.

demonstrates the impressive rigidity and degree of preorganization of ligand **L1** for the final macrocyclization processes that lead to $[M_2(\mathbf{L1})_2]^{2+}$, despite a Cu···Cu intrahelical distance of 13.9 Å (Figure 2), which is much larger than that found in the helicate reported by Lehn and co-workers (5.8 Å).[12b] Moreover, this result justifies the hypothesis of how the optimized preorganization concept $c_{M,Lk}^{eff} = c_{M,L1}^{eff}(d_k/d_1)^{-3}$ can be used in order to limit the number of microscopic descriptors (see Appendix 2 in the Supporting Information).[13]

However, the most striking results of this work concerns the intramolecular intermetallic parameters, which lead to greater repulsion with increasing intermetallic distance, according to the empirical quadratic trend ($\Delta E_{\mathbf{L1},d=1.4nm}^{Cu,Cu} = 11\ kJ\,mol^{-1} < \Delta E_{\mathbf{L2},d=1.8nm}^{Cu,Cu} = 20\ kJ\,mol^{-1} < \Delta E_{\mathbf{L3},d=2.2nm}^{Cu,Cu} = 33\ kJ\,mol^{-1}$ and $\Delta E_{\mathbf{L1},d=1.4nm}^{Ag,Ag} = -14\ kJ\,mol^{-1} < \Delta E_{\mathbf{L2},d=1.8nm}^{Ag,Ag} = 2\ kJ\,mol^{-1} < \Delta E_{\mathbf{L3},d=2.2nm}^{Ag,Ag} = 22\ kJ\,mol^{-1}$; Figure S5 in the Supporting Information).[14] An approach for the chemical rationalization and tuning of these interactions requires the combination of charge repulsion [Coulomb equation; Eq. (1)] and changes in solvation energies [Born equation; Eq. (2)]. If we consider the simple ligand-exchange reaction shown in the thermodynamic Born–Haber cycle depicted in Figure 3, we immediately notice that $\beta_{exch}^{\mathbf{L1},\mathbf{Lk}} = \beta_{2,2}^{M,\mathbf{Lk}}/\beta_{2,2}^{M,\mathbf{L1}}$, and the subsequent introduction of twice Equation (9) leads to Equation (11), which ultimately transforms into Equation (12) by use of the standard van't Hoff isotherm (standard state = 1M),[15] and the definitions of $u^{M,M}$ and $u^{L,L}$ (Table 2).

$$\beta_{exch}^{\mathbf{L1},\mathbf{Lk}} = \frac{\beta_{2,2}^{M,\mathbf{Lk}}}{\beta_{2,2}^{M,\mathbf{L1}}} = \frac{u_{\mathbf{Lk}}^{M,M}}{u_{\mathbf{L1}}^{M,M}}\left(\frac{d_k}{d_1}\right)^{-3} \tag{11}$$

$$\Delta G_{exch}^{\mathbf{L1},\mathbf{Lk}} = -RT\ln(\beta_{exch}^{\mathbf{L1},\mathbf{Lk}}) = \Delta E_{\mathbf{Lk}}^{M,M} - \Delta E_{\mathbf{L1}}^{M,M} + 3RT\ln(d_k/d_1) \tag{12}$$

In the gas phase, $\Delta G_{exch,gas}^{\mathbf{L1},\mathbf{Lk}}$ can be easily estimated because $\Delta E_{Lk,gas}^{M,M}$ ($k = 1$–3) are simply given by the Coulomb equation [Eq. (1)]. The use of the Born equation [Eq. (2)] for approximating the solvation energies of the charged complexes $\Delta_{solv}G^0_{M_2(\mathbf{L1})_2}$ and $\Delta_{solv}G^0_{M_2(\mathbf{Lk})_2}$, followed by application to the Born–Haber cycle shown in Figure 3, eventually gives Equations (13)–(16), which correlate the apparent difference in intermetallic interactions observed in solution $\Delta E_{\mathbf{Lk},sol}^{M,M} - \Delta E_{\mathbf{L1},sol}^{M,M}$ with various chemically accessible parameters (Appendix 3 in the Supporting Information).

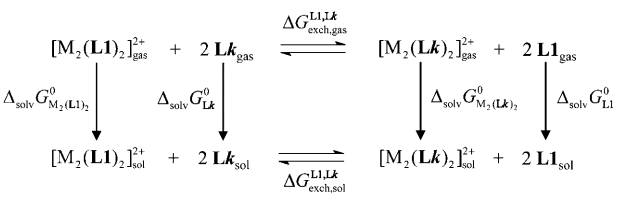

Figure 3. Thermodynamic Born–Haber cycle for ligand exchange reactions of **L1** with **Lk** ($k = 2$, 3) in the binuclear double-stranded helicates $[M_2(\mathbf{L1})_2]^{2+}$.

$$\Delta E_{\mathbf{Lk},sol}^{M,M} - \Delta E_{\mathbf{L1},sol}^{M,M} = \Delta\Delta G_{Coulomb}^{\mathbf{L1},\mathbf{Lk}} + \Delta\Delta_{solv}G_{complex}^{\mathbf{L1},\mathbf{Lk}} + 2\Delta\Delta_{solv}G_{ligand}^{\mathbf{L1},\mathbf{Lk}} \tag{13}$$

with

$$\Delta\Delta G_{Coulomb}^{\mathbf{L1},\mathbf{Lk}} = \frac{z_1 z_2 e^2 N_{Av}}{4\pi\varepsilon_0}\left(\frac{1}{d_k} - \frac{1}{d_1}\right) \tag{14}$$

and

$$\Delta\Delta_{solv}G_{complex}^{\mathbf{L1},\mathbf{Lk}} = -\frac{(z_1+z_2)^2 e^2 N_{Av}}{8\pi\varepsilon_0}\left(1 - \frac{1}{\varepsilon_r^{solv}}\right)\left(\frac{1}{R_k} - \frac{1}{R_1}\right) \tag{15}$$

and

$$\Delta\Delta_{solv}G_{ligand}^{\mathbf{L1},\mathbf{Lk}} = \Delta_{solv}G_{\mathbf{L1}}^{0} - \Delta_{solv}G_{\mathbf{Lk}}^{0} \tag{16}$$

The first negative term shown in Equation (14) ($d_k > d_1$) simply measures the decreased electrostatic intermetallic repulsion that accompanies the larger separation between the metals when **L1** is replaced with **Lk** ($k = 2$, 3). The second positive contribution in Equation (15) ($R_k > R_1$) results from the decreased solvation energies that accompany the increasing size of the complex when **L1** is replaced with **Lk** ($k = 2, 3$). Once the charge of the metals are fixed ($z_1 = z_2 = 1$ for $M = Cu^I$, Ag^I), we can reasonably assume identical charge polarization in the three complexes with ligands **L1** to **L3**. The contribution of the Coulomb equation thus exclusively relies on changes in intermetallic distance, while that of the solvation depends on variations in global shapes and sizes of the complexes that result from the changes in intermetallic distances. Finally, the last term in Equation (16) simply corresponds to the difference in the solvation free energies of the free ligands, a difference which is often of very small magnitude for such closely related ligands.[9] A rough quantitative calculation with point charge Equation (13) (Table 3) assumes 1) $\Delta\Delta_{solv}G_{ligand}^{\mathbf{L1},\mathbf{Lk}} \approx 0$, 2) metal polarization is identical in the three binuclear complexes and is neglected as a first approximation because it only corresponds to a scaling factor (i.e., $z_1 = z_2 = 1$ for $[M_2(\mathbf{Lk})_2]^{2+}$), 3) the intermetallic separation is taken as the value of d_k estimated from the model structures (Figure 2), and 4) the pseudo-spherical radii R_k of the complexes in solution are estimated by their experimental hydrodynamic radii (Table S1 in the Supporting Information).[16]

Table 3: Experimental intermetallic interactions $\Delta E^{M,M}_{\mathbf{Lk},sol}$ and differences $\Delta\Delta E^{M,M}_{sol,exp}$ for complexes $[M_2(\mathbf{Lk})_2]^{2+}$.[a]

Ligand	$\Delta E^{Cu,Cu}_{\mathbf{Lk},sol}$ [kJ mol^{-1}]	$\Delta\Delta E^{Cu,Cu}_{sol,exp}$ [kJ mol^{-1}]	$\Delta\Delta E^{Cu,Cu}_{sol,calcd}$ [kJ mol^{-1}]	$\Delta E^{Ag,Ag}_{\mathbf{Lk},sol}$ [kJ mol^{-1}]	$\Delta\Delta E^{Ag,Ag}_{sol,exp}$ [kJ mol^{-1}]	$\Delta\Delta E^{Ag,Ag}_{sol,calcd}$ [kJ mol^{-1}]
L1	11	0	0	-14	0	0
L2	20	9	26	2	16	7
L3	33	22	49	22	36	17

[a] $\Delta E^{M,M}_{\mathbf{Lk},sol}$ given in Table 2. $\Delta\Delta E^{M,M}_{sol,exp} = \Delta E^{M,M}_{\mathbf{Lk},sol} - \Delta E^{M,M}_{\mathbf{L1},sol}$ for complexes $[M_2(\mathbf{Lk})_2]^{2+}$ (M = Cu^{I}, Ag^{I}; k = 1–3) in dichloromethane/acetonitrile (5:1) at 293 K compared with $\Delta\Delta E^{M,M}_{sol,calcd}$ computed with Equation (13).The assumptions for the application of Equation (13) are given in the text.

Despite the rough approximations used for this simple calculation, we notice that Equation (13) indeed reproduces the counterintuitive trend $\Delta E^{M,M}_{\mathbf{L1},d=1.4nm} < \Delta E^{M,M}_{\mathbf{L2},d=1.8nm} < \Delta E^{M,M}_{\mathbf{L3},d=2.2nm}$ since $\Delta\Delta E^{M,M}_{sol,calcd} = \left(\Delta E^{M,M}_{\mathbf{Lk},sol} - \Delta E^{M,M}_{\mathbf{L1},sol}\right)_{calcd}$ are positive and systematically grow with the size of **L*k*** (Table 3). Moreover, the discrepancy between experimental and computed values for $\Delta\Delta E^{M,M}_{sol}$ is surprisingly small compared with the large and opposing contributions brought by the Coulomb and solvation processes. We are aware that the point charge model used in Equations (1) and (2), which is further implemented in the thermodynamic Born–Haber cycle, can be greatly improved with modern computing techniques.[9] However, its analytical form shown in Equations (13)–(16) may greatly help synthetic, coordination, or supramolecular chemists to feel the structural and electronic possibilities offered by this simple model for tuning the nature and stabilities of their final self-assembled complexes. For the double-stranded helicates $[M_2(\mathbf{Lk})_2]^{2+}$ considered here, the solvation contribution dominates the coulombic contribution, and the intermetallic interactions increasingly destabilize the complexes that have a larger intermetallic separation. However, Equation (13) suggests that this trend is not unavoidable, and we can predict that an increase of the volume of the spacer will result in effects with comparable powers, or even with an inverted sequence. The latter borderline behavior has been previously observed for polynuclear lanthanide helicates (Figure 1),[9] and the most important conclusion of the present work thus concerns our understanding of the apparent intermetallic interactions in solvated polynuclear complexes. These interactions, which are not inevitably repulsive, can be modulated by the programmable contribution of the solvation energies.

Received: August 19, 2009
Published online: November 30, 2009

Keywords: coulombic interactions · helical structures · intermetallic interactions · self-assembly · solvation effects

[1] a) J. D. Dunitz, A. Gavezzotti, *Acc. Chem. Res.* **1999**, *32*, 677; b) E. O. Purisima, T. Sulea, *J. Phys. Chem. B* **2009**, *113*, 8206.
[2] B. Baytekin, H. T. Baytekin, C. A. Schalley, *Org. Biomol. Chem.* **2006**, *4*, 2825.
[3] a) J. S. Fleming, E. Psillakis, S. M. Couchman, J. C. Jeffery, J. A. McCleverty, M. D. Ward, *J. Chem. Soc. Dalton Trans.* **1998**, 537; b) J. C. Jeffery, C. R. Rice, L. P. Harding, C. J. Baylies, T. Riis-Johannessen, *Chem. Eur. J.* **2007**, *13*, 5256; c) C. J. Baylies, L. P. Harding, J. C. Jeffery, R. Moon, C. R. Rice, T. Riis-Johannessen, *New J. Chem.* **2007**, *31*, 1525; d) S. Hiraoka, M. Goda, M. Shionoya, *J. Am. Chem. Soc.* **2009**, *131*, 4592.
[4] G. Canard, C. Piguet, *Inorg. Chem.* **2007**, *46*, 3511.
[5] R. H. Stokes, *J. Am. Chem. Soc.* **1964**, *86*, 979.
[6] N. Dalla Favera, L. Guénée, G. Bernardinelli, C. Piguet, *Dalton Trans.* **2009**, 7625
[7] J. Hamacek, M. Borkovec, C. Piguet, *Dalton Trans.* **2006**, 1473.
[8] G. Ercolani, C. Piguet, M. Borkovec, J. Hamacek, *J. Phys. Chem. B* **2007**, *111*, 12195.
[9] T. Riis-Johannessen, N. Dalla Favera, T. Todorova, S. M. Huber, L. Gagliardi, C. Piguet, *Chem. Eur. J.* **2009**, *15*, 12702
[10] U. Kiehne, T. Weilandt, A. Lützen, *Org. Lett.* **2007**, *9*, 1283.
[11] J. Garcia De La Torre, *Biophys. Chem.* **2001**, *94*, 265.
[12] a) J. Hamacek, M. Borkovec, C. Piguet, *Chem. Eur. J.* **2005**, *11*, 5227; b) J.-M. Lehn, A. Rigault, J. Siegel, J. Harrowfield, B. Chevrier, D. Moras, *Proc. Natl. Acad. Sci. USA* **1987**, *84*, 2565.
[13] a) J. M. Gargano, T. Ngo, J. Y. Kim, D. W. K. Acheson, W. J. Lees, *J. Am. Chem. Soc.* **2001**, *123*, 12909; b) N. Dalla-Favera, J. Hamacek, M. Borkovec, D. Jeannerat, F. Gumy, J.-C. G. Bünzli, G. Ercolani, C. Piguet, *Chem. Eur. J.* **2008**, *14*, 2994.
[14] Although not directly relevant to the main topics of this Communication, the increased intermetallic repulsion competes with anti-cooperative interligand interactions in $[M_m(\mathbf{Lk})_n]^{m+}$, which explains the detection of $[M_2(\mathbf{Lk})]^{2+}$ as the minor complex when $\Delta E^{M,M}_{\mathbf{Lk}} < \Delta E^{L,L}$ [k = 1, 2, Eq. (8), Table 1] and $[M(\mathbf{L3})_2]^{+}$ as the minor complex when $\Delta E^{M,M}_{\mathbf{L3}} > \Delta E^{L,L}$ [Eq. (10), Table 1].
[15] D. Munro, *Chem. Br.* **1977**, *13*, 100, and references therein.
[16] The hydrodynamic radii of $[M_2(\mathbf{L3})_2]^{2+}$ are estimated by a linear extension $R_k = a - b\,d_k$ parameterized with the experimental values found for R_1 and R_2 (Table S1 in the Supporting Information). We found $R_3^{Cu} = 8.47$ Å and $R_3^{Ag} = 8.03$ Å.

